A step toward lifting the fog off mist explosions: Comparative study of three fuels

Stephanie El – Zahlanieh, Shyarinya Sivabalan, Idalba Souza dos Santos, Benoit Tribouilloy, David Brunello, Alexis Vignes, Olivier Dufaud

A step toward lifting the fog off mist explosions: Comparative study of three fuels

Stephanie El – Zahlanieh[a,b], Shyarinya Sivabalan[a], Idalba Souza Dos Santos[a], Benoit Tribouilloy[b], David Brunello[a], Alexis Vignes[b] and Olivier Dufaud[a]

[a] Reactions and Chemical Engineering Laboratory (LRGP), Lorraine University, UMR 7274 CNRS, 1, rue Grandville, BP 20451, 54001, Nancy, France

[b] INERIS, Fire, Dispersion and Explosion Division, Parc Technologique ALATA, BP 2, F-60550, Verneuil-en-Halatte, France

stephanie.el-zahlanieh@univ-lorraine.fr

olivier.dufaud@univ-lorraine.fr

Abstract

Gases, vapors, and dusts are all potential explosion threats; however, mists should also be taken into account. Indeed, dozens of accidents involving hydrocarbon mists were identified in incident surveys. Mist explosions continue to occur, highlighting the need to evaluate and assess the validity of present approaches for assessing mist ATEX risks and to establish reliable standardized safety parameters for fuel mists.

In a modified apparatus based on the 20L explosion sphere, three fluids of industrial interest were investigated. A new siphon injection system comprising a Venturi junction was installed, offering a wide range of dispersion performances. This system was controlled by a specifically developed program, ensuring the apparatus's versatility and adaptability to various tested liquids. It enables precise control of the gas carrier flow, liquid flow, and injection and ignition durations, allowing modification of the dilution rate of a particular droplet size distribution (DSD). The mist cloud dispersed in the 20 L sphere was characterized by determining its DSD using an in-situ laser diffraction sensor and by performing Particle Image Velocimetry (PIV). Mists of kerosene, diesel and ethanol were then subjected to tests to assess their lower explosive limit (LEL_{mist}), minimum ignition energy (MIE), maximum explosion pressure (P_{max}), and rate of pressure rise (dP/dt_{max}). For instance, it was found that the LEL_{mist} of ethanol, kerosene Jet A1, and diesel fuel for a DSD averaged at 8 – 10 µm reach 77, 94, and 93 g/m^3 respectively. This LEL_{mist} was also shown to increase with increasing DSD in the case of Jet A1 mists. A sensitivity study was also performed to emphasize the impact of parameters such as the fuel type, the DSD, and the mist temperature. Findings showed that the explosion severity is strongly influenced by the chemical nature and the volatility of the dispersed fuel. Moreover, controlling the sphere temperature was proven to be a

crucial step when using such apparatus for the evaluation of the explosibility of mists. An evaporation model based on the d^2 law was also developed to visualize the vapor-liquid ratio before ignition. These findings have already led to the development of a new procedure for determining safety standards for hydrocarbon mists, as well as tools to assess mist explosion risks. They have proven that it is possible to evaluate the ignition sensitivity and explosion severity of fuel mists using a single well-known apparatus.

Keywords: *Process Safety, Fuels, Risk Assessment, Hazardous Areas, Hydrocarbon Aerosols, Explosion*

Nomenclature:

B_T, B_M	:	Thermal and mass transfer Spalding numbers
c_{pv}	:	Heat capacity of the vapor phase
D_x	:	Diameter where x percent of the distribution has a smaller droplet size
d_0	:	Initial droplet diameter
K	:	Vaporization rate of the fuel
Le	:	Lewis number
L_v	:	Enthalpy of vaporization
N	:	Number of droplets
Q	:	Combustion enthalpy
Re	:	Reynolds number
P_m	:	Maximum explosion pressure at a specific fuel concentration
P_{max}	:	Maximum value of the maximum explosion pressures
dP/dt_m	:	Maximum rate of pressure rise at a specific fuel concentration
dP/dt_{max}	:	Maximum value of the maximum rates of pressure rise

s	:	Mass stoichiometric coefficient
Sc	:	Schmidt number
SMD	:	Sauter mean diameter
T_d	:	Droplet temperature
T_∞	:	Temperature of the environment
u	:	Horizontal velocity
v	:	Vertical velocity
v_{rms}	:	Root-mean-square velocity
x_i'	:	Property fluctuation
$\bar{x}$	:	Mean property
$Y_{Ox,\infty}$	:	Oxygen mass fraction
Y_{vs}	:	Mass fraction at the droplet surface
$Y_{v\infty}$	:	Mass fraction in the surrounding gases
ρ	:	Density

1 Introduction

In the chemical and petrochemical industries, various processes are susceptible to lead to the formation of flammable hydrocarbon aerosols under certain conditions (Lees et al., 2019). These unintended generations of hydrocarbon mists, when compared to gases or dust clouds, tend to receive less attention and seem more complicated to understand (Yuan et al., 2021). Nevertheless, such releases may ignite and give rise to dangerous explosions. Dozens of such explosions have been reported throughout the years despite the efforts taken to mitigate such incidents. Studies and incident reviews focusing on these hazards date back to the early 1950s when Eichhorn shed light

on such matter in one of his publications in the Petroleum Refiner entitled “Careful! Mist can explode” (Eichhorn, 1955). The author has since introduced the possibility of mists igniting at temperatures well below their flashpoints. A few years later, in 1995, Eckhoff published a literature survey in which the author reviewed studies concerning the generation, ignition, combustion, and explosion of ignitable mists (Eckhoff, 1995). Interest in such a crucial subject has, since then, grown throughout the years. For instance, in 2009, Santon (2009) published an incident survey reporting 37 mist incidents, among which 9 explosions lead to 29 fatalities. Ten years later, Lees et al. (2019) notably showed that 10% of reported releases on offshore oil and gas installations in the United Kingdom involved sprays or mists. More recently, a comprehensive review was performed by Yuan et al. (2021) and led to the proposal of a systematic strategy to investigate aerosol explosion, which is in full accordance with the work presented here.

To better understand the phenomenon of fuel mist explosions, the mist cloud should be well defined and characterized. According to the Globally Harmonized System of classification and labelling of chemicals (GHS) (ST/SG/AC.10/30/Rev.8, 2019), mists are defined as liquid droplets, generally of sizes ranging from 1 to about 100 µm, of a certain substance or mixture suspended in a gas - usually air. The alternative term “smoke” is then used for aerosols with diameters lower than 1 µm (Fraser and Eisenklam, 1956), while “sprays” consist of dispersed droplets of diameters generally greater than 50 µm. Other definitions are also encountered. For instance, Ballal and Lefebvre (1981) consider the term "mist" to be suitable up to 100 µm (Gant, 2013). Nevertheless, as proposed by Eckhoff (2016), the terms “spray” and “mist” are used arbitrarily in this paper as they are both relevant in this case.

Even though many measures, such as the installation of mist detectors, exist to prevent mist explosions, their ongoing occurrence demonstrates the need to assess the relevance of the current

approaches for the evaluation of the mist explosion risks. Indeed, the importance of hazardous area classification (HAC), as well as the lack of tools which correlate the dispersion of mists with their flammability and explosion severity, is abundantly expressed in literature (Gant, 2013; Yuan et al., 2021). For instance, European ATEX regulations require assessing the risk of formation and ignition of explosive atmosphere (ATEX) associated with the production of a flammable mists. Nevertheless, due to the lack of tools, risk analysis and area classification prove difficult. This lack of knowledge is clearly highlighted in some guides such as the EI15 (Energy Institute, 2015) in which it is stated that "there is little knowledge on the formation of flammable mists and the appropriate extents of associated hazardous areas".

In order to mitigate the occurrence of such explosions and to assess the flammability and explosion severity of hydrocarbon mists, the factors and criteria of liquid handling, as well as the safety parameters of fluids should be identified. If such definitions are achieved, the classification of hazardous areas (HAC) would be a step closer for mists, and the improvement of current ATEX standards and regulatory provisions concerning mists would then be achievable. In other words, "lifting the fog off fuel mist explosions" may finally be possible.

In this study, different fluids with a high industrial interest were selected to be tested in a new apparatus based on the standardized 20 L explosion sphere. The generated mist was characterized, notably by its droplet size distribution and its turbulence, and explosion tests were performed to determine the lower explosive limit (LEL_{mist}), the minimum ignition energy (MIE), the maximum explosion pressure (P_{max}) and the maximum rate of pressure rise (dP/dt_{max}) of hydrocarbon mists. The main goals of this work are i) to demonstrate, through some examples, that it is possible to characterize the flammability and explosion severity of mists using modified standard set-ups such as the 20 L sphere, ii) to show the influence of some operating conditions on the safety parameters

of hydrocarbon mists. It can hence be stated that this study aims to provide tools for control banding based on an already-standardized set-up used for gases and dusts which ensures the ability to compare and propose ample solutions for explosion risk management while representing industrial conditions. Ji et al. (2021) clearly show that such risk assessment can only be done by identifying and considering the major factors influencing the liquid aerosol flammability. To cover a wide range of industrial conditions the following parameters were varied: turbulence level, ignition energy, initial temperature, droplet size distribution and mist concentration.

2 Materials and Methods

2.1 Fuel selection

A large variety of fuels has been involved in mist explosion incidents, ranging from vegetable oils to hydraulic oils and crude oils (Santon, 2009). During an oil mists Joint Industry Project (JIP) led by the Health and Safety Executive (HSE) (Burrell and Gant, 2017), a list of fluids was proposed comprising fuels of industrial interest and specific physicochemical properties. In addition, based on the properties that were identified to be the most affecting on oil mist hazards, a fluid classification system was developed by the Health and Safety Executive. This system divided the chosen fluids into four release classes based on their flashpoint and their ease of atomization, a parameter represented by the Ohnesorge number. For this paper, three fuels were chosen to be studied under certain conditions: ethanol, Jet A1 kerosene and diesel fuel. The choice of each fluid can be justified by both industrial and scientific considerations.

Ethanol

The industrial value of ethanol is continuously growing throughout the years with its emergent use as an engine fuel or fuel additive for automobiles. Such demand for ethanol or ethanol-fuel blends is and will keep leading to an increase in its production and transport, hence increasing the requirements to manage fire or explosion risks. Moreover, the high volatility of ethanol leads to its rapid evaporation near the flame kernel when dispersed in small droplets which justifies the comparison with ethanol vapor explosion results. It should be noted that mist characterization tests at ambient temperature are represented in this study for ethanol, but tests on the following two fluids were also performed.

Jet A1 kerosene

In 2009, Santon showed that 7 incidents over 29 detailed in his review, were related to kerosene mists. They were mostly related to transportation activities, from cargo accidents to aviation kerosene explosions (Santon, 2009). Filling or emptying (voluntarily or accidentally) of storages must also be carefully examined with regard to aerosols generation. For instance, kerosene explosions occurred in Cilacap (1995) and Mombasa (2013) during tank refueling and storage leaking, respectively. Bowen and Shirvill (1994) also pointed out the risks behind the potential atomization of kerosene.

Diesel fuel

In their incident review, Lees et al. (2019) mentioned that data from the UK Hydrocarbon Release Database (HCRD) showed that 20% of mist reported incidents took place from diesel sources. In fact, the authors stated that out of 48 mist/spray release flash fires reported between 2000 and 2005, 11 involved diesel releases.

Table 1 shows the main physicochemical properties of the selected fuels. It should be highlighted that the Ohnesorge number (Oh), used for the HSE classification, represents the ratio between the viscous forces to surface tension and inertial forces, i.e., at a given Reynolds number, increasing Oh will improve liquid atomization.

Although diesel fuel has similar physicochemical properties to that of kerosene Jet A1 and is categorized in the same HSE release class, the slight differences, notably the flashpoint and vapor pressure, were proven to lead to different behaviors during their evaporation and once ignited.

Table 1. Physicochemical properties of the three selected fuels

Properties	Ethanol 96%*	Aviation fuel Jet A1**	Diesel***
Flashpoint (°C)	13-17	≥ 38	> 52
Density (kg/m^3)	790	750 – 840	750 – 850
Viscosity (cSt)	1.2	8	2 – 4.5 @ 40°C ◆
Surface Tension (kg/s^2)	0.022	0.026	0.027
HSE Release Class	'Unclassified'	Class I (Oh ratio ≥ 2, Flashpoint < 125°C)	Class I (Oh ratio ≥ 2, Flashpoint < 125°C)
Flammability limits (%)	3.3 – 19	0.6 – 6	0.5 – 8
Auto-ignition temperature (°C)	363	210	232 – 260

** MSDS from ThermoFisher Scientific ** MSDS from Neste *** MSDS from Hollyfrontier ◆BS EN 590*

2.2 Mist generation system

The accidental formation of an explosive flammable mist cloud can be caused by several phenomena. For instance, it can be due to the evaporation of fuels in heated areas, their subsequent circulation, and then their condensation in colder areas (Eckhoff, 1995). In addition, leaks or ruptures due the damages or corrosion in vessels and pipelines can lead to high pressure releases and hydrocarbon mist generation. To better represent a spray or mist caused by a leak or rupture, various generation methodologies could be adopted. The wide use of sprays in industrial applications lays out several options to choose from. Nevertheless, the experimental procedure proposed to characterise the ignition sensitivity and explosion severity of mists aims to be standardized, so that the results can be compared and that generic safety measures can be proposed. Therefore, the selected generation system should be easy to find and implement but should also be able to mimic "idealized" conditions of a mist release.

In this work, a siphon/gravity-fed set-up comprising a Venturi junction with two inlets (an air inlet and a liquid inlet) was used to generate mist. The main component of this generation system is a spray nozzle set composed of a fluid cap and an air cap (Spraying Systems) through which the liquid/air jet passes and fragments. Mist/spray generation was investigated as a function of three relevant parameters stated by Kooij et al. (2018): nozzle type, spraying pressure and fluid properties. Three nozzle sets of different orifice diameters were chosen to represent three ranges of droplet size distribution (Figure 1). In addition to the nozzle set, the air injection pressure, which shows an important influence on the droplet size, was varied at least between 2 and 5 bar. These pressures were chosen according to the maximum pressure tolerance of the three nozzle sets.

Figure 1. The three spray nozzle sets, from left to right: N1, N' and N2

2.3 Mist characterization

Gant (2013) pointed out that characterizing a mist properly before its ignition is of great importance since the safety parameters of mists are highly affected by their droplet size distribution, concentration, and turbulence. These three parameters are studied by using an in-situ diffraction laser sensor as well as by implementing Particle Image Velocimetry (PIV).

2.3.1 Droplet Size Distribution

The time evolution of droplet size distributions was determined by in-situ laser diffraction (Helos/KR-Vario by Sympatec GmbH) and will be later supplemented by APS spectroscopy (aerodynamic diameter measurement - TSI) to characterize the submicron droplets. The Helos laser sensor used for such measurement is designed to analyse the droplet size by using 3 high-resolution measuring ranges (R1, R3 and R5) from 0.5 µm to 875 µm. The apparatus measures the droplet size distribution (DSD) directly through the transparent windows (borosilicate glass) of a modified 20L open sphere similar to the standard explosion vessel (Santandrea et al., 2020). The

R3 lens was mainly used during this study as it covers a range of droplet diameters from 0.5/0.9 µm to 175 µm. The acquisition frequency was set to 2 distributions per millisecond. The measurements given by the sensor are notably the volume diameter d_{10}, d_{50}, d_{90} and the $D_{3,2}$ (Sauter Mean Diameter, SMD). It should be underlined that Krishna et al. (2003) stated that SMD, diameter of a droplet having the same volume/surface area ratio as the aerosol, is the most common mean diameter to consider for aerosols dispersion, heating or combustion. In order to have an approximation of the DSD near the kernel spark produced by an ignition source described in more detail in Section 2.4, the height of the sensor was adjusted to a height corresponding to the location of the ignition source.

2.3.2 Particle Image Velocimetry

Using the same modified 20 L vessel, PIV experiments were performed under different conditions to measure the level of turbulence reached by the generated mist cloud. In fact, both DSD time-evolution and explosion severity are considerably affected by the turbulence of the mixture (Skjold, 2003). To perform such tests, Neodym-Yttrium-Aluminum-Garnet (Nd:YAG) was used to generate a continuous wave laser sheet of a wavelength of 532 nm described in detail in Torrado (2017). The dispersed droplets would then be illuminated allowing the tracking and the analysis of their movements. A high-speed video camera (Phantom VEO 410L) was used to record the flow of the droplets in videos of 2000 frames per second. To analyze the recorded videos, an open-source software PIVlab 2.45 (Thielicke, 2021) was used to perform image preprocessing, PIV analysis using interpolation methods, calibration, post-processing, and data validation. From the data acquired from PIVlab, the mean velocities $\bar{u}$ and $\bar{v}$, as well as the horizontal and vertical velocity fluctuations u_i' and v_i' (equation 1 and 2), were estimated allowing the calculation of the

root-mean-square velocity (v_{rms} – equation 3) which physically characterizes the turbulence kinetic energy.

$$u_i' = u - \bar{u} \quad (1)$$

$$v_i' = v - \bar{v} \quad (2)$$

$$v_{rms} = \sqrt{\frac{1}{N}\sum (u_i')^2 + \frac{1}{N}\sum (v_i')^2} \quad (3)$$

where u_i' is the horizontal velocity fluctuation, v_i' is the vertical velocity fluctuation and N is the number of droplets detected for the velocity estimation.

2.4 Ignition sources

Potential ignition sources in accidental fires or explosions can vary from electrical discharges or sparks to hot surfaces or to malfunctioning electrical circuits. In previous studies on explosion limits and deflagration pressures, ignition sources such as exploding wire ignitors, spark ignition, pyrotechnical ignitors, and hot spot ignitors have been used (Ballal and Lefebvre, 1981; Yuan et al., 2019; Zheng et al., 2014).

For this study, wide ranges of energies, starting from 1 mJ, were required. Therefore, both spark ignition as well as chemical pyrotechnical ignitors were chosen. In tests performed with spark ignition, two stainless steel electrodes were placed in the center of the 20 L explosion sphere with a separating distance of 6 ± 0.1 mm. The electrodes were insulated from the sphere's wall using Teflon plugs. Both electrodes were connected to a KSEP 320 high voltage unit, which was also

bypassed by a custom control system. The maximum power generated by such system is 225 W, i.e., 225 J/s. Hence, to deliver an energy of 100 J, a permanent spark would be generated during 444 milliseconds.

To avoid generating a spark for a long duration which may lead to the sedimentation of droplets, permanent spark ignition was only used up to energies of 100 J. For higher energies, chemical pyrotechnical ignitors (Sobbe GmbH) of energies ranging from 100 J to 10 kJ were used. These ignitors were actuated electrically by a low-voltage electrical signal sent by the KSEP 310 unit. Both ignition sources were compared at 100 J to ensure that they both deliver approximate results.

2.5 Mist flammability and explosion severity

The standard 20 L explosion sphere used for dust explosion tests was modified to become the Modified 20 L Ignition and explosion Severity Test device (MIST). The modifications made comprised the installation of the mist generation system at the bottom of the sphere using a custom-made adapted support, the removal of the dust container, as shown in the Figure 2, and the installation of two electronic valves to control the inlet flowrates as well as the liquid/air ratio. The flowrates were found to range between 0.25 and 0.29 g/s for nozzle set N1 depending on the type of the liquid and increase to about 1 and 1.1 g/s for nozzle sets N' and N2 respectively at an injection pressure of 3 bar. Before injecting the fuel/air mixture, the sphere was partially vacuumed to a calculated pressure, so that, when the mist was fully injected, an atmospheric pressure would be attained. The two ignition sources mentioned in Section 2.4 were used for this test with an ignition delay t_v (time between the end of injection and the start of ignition) set to 1 ms, which can be considered as negligible. The control of the system as well as the acquisition

of the data were performed using a new control system and a LabView program developed during this work. This system controls the KSEP 310 and 332 units (Cesana AG), the inlet electronic valves (gas and liquid) and allows a safe operation of the test equipment and an optimum evaluation of the explosion results with an acquisition frequency of 5000 measurements per second. Explosion tests were performed thrice and the standard deviation was represented by error bars on graphs.

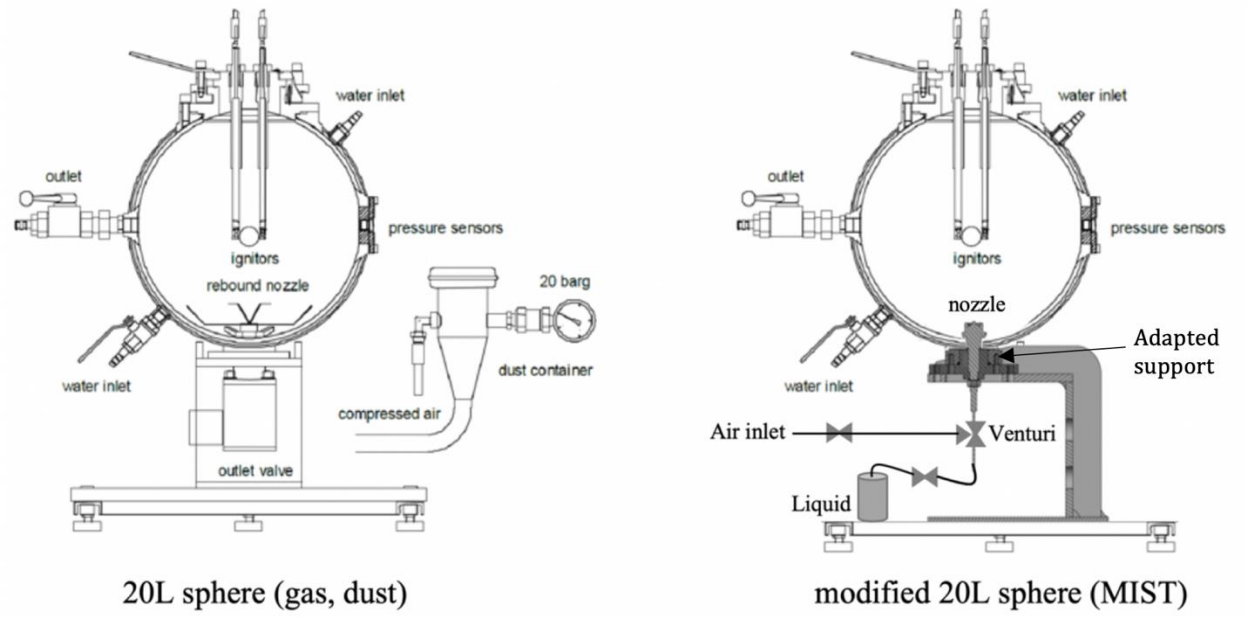

Figure 2. Modification of the standardized 20L explosion sphere. Left: standard 20 L sphere – Right: modified 20L sphere (MIST)

3 Results and Discussion

3.1 Mist characterization

3.1.1 Droplet Size Distribution

Mists were generated in the open 20L sphere using the three nozzle sets presented in Section 2.2. DSD measurements were performed during a 4-second generation period and up to 1 second after the closure of the valves, with intervals of 50 ms (2 DSD per ms and an average value each 50 ms). As it is shown in Figure 3 for ethanol, three ranges of droplet diameters can be obtained by changing the nozzle set. Nevertheless, it should be noted that with nozzle sets N' and N2, a peak corresponding to smaller diameters (between 6 and 18µm) was always observed, demonstrating the persistence of 'primary droplets' for nozzle set N' and of a fragmentation phenomenon for N2. It should be noticed that, in the case of mist generation through the N' nozzle set, hybrid mixtures (vapor – liquid phase) can be created during the ignition step due to the presence of fine droplets being easily vaporized along with larger droplets.

Since the properties of fluids are one of the many relevant parameters affecting the droplet size distribution of a mist (Kooij et al., 2018), a sensitivity study has been undertaken to study the influence of preheating or pressurizing the liquid on the DSD. A metallic reservoir that holds up to 10 bar of internal pressure and 100 °C was designed to store the liquid hydrocarbons. Granulometry tests were also performed on kerosene Jet A1 and diesel fuel mists and demonstrated similar DSDs as these shown in Figure 3. Table 2 also shows the DSD of the three fluids at the end of a four-second injection with an air pressure of 3 bar, a condition under which most of the presented experiments were performed.

Table 2. Droplet size distribution characteristics at t = 4000 ms of the three fuels using nozzle set N1

P_{inj} = 3 bar

Nozzle set	Ethanol			Kerosene Jet A1			Diesel		
N1	D_{50} (µm)	SMD (µm)	D_{90} (µm)	D_{50} (µm)	SMD (µm)	D_{90} (µm)	D_{50} (µm)	SMD (µm)	D_{90} (µm)
	9.7	9.4	12.2	7.3	7.3	10.5	8.5	8.3	11.4

Being able to independently control the DSD and the flow (i.e. the fuel equivalence ratio) is an essential point of any study on the risks associated with mists. This will allow to control and study the effect of the fuel equivalence ratio, the droplet size distribution and the chemical nature of the fuel, and to determine their impact on the ignition sensitivity and the explosion severity of hydrocarbon mists.

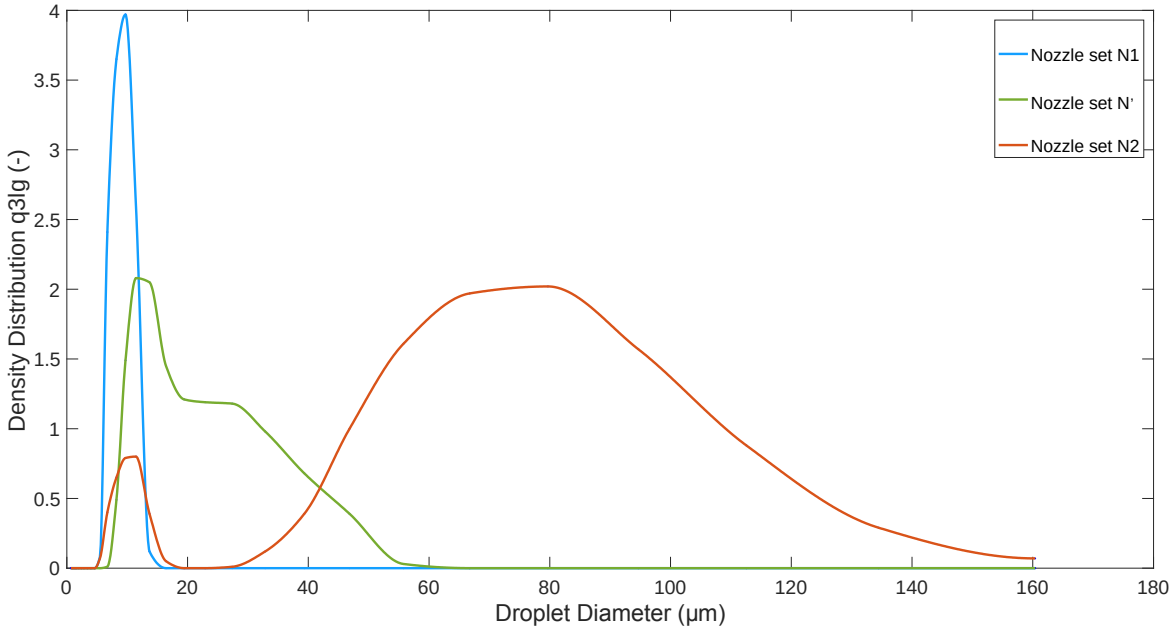

Figure 3. Droplet size distribution (volume/mass) at t = 3000 ms of ethanol mist generated at P = 2 bar using the three nozzle sets

3.1.2 Particle Image Velocimetry

Figure 4 exhibits the spatial variation of the velocity magnitude of ethanol droplets at the end of the mist generation at an air injection pressure of 3 bar and after an injection time of 1 second using nozzle set N'. Measurements were carried out for just 1-second generations to maintain precision and visibility of the illuminated droplets. Velocity magnitudes ranging from 0.5 to 5.5 m/s were attained at the end of the injection, but much higher values were reached during injection. As for the vertical and horizontal velocity vectors, absolute values as high as 14 m/s and 8 m/s respectively were reached. Using equation (3), values of about 1.5 m/s of the root-mean square velocity (v_{rms}) were reached at the end of the mist generation. This v_{rms} reached a maximum of 1.94 m/s at t_{inj} = 200 ms. Turbulence calculations were also performed 1 ms after the end of the injection to visualize the turbulence level at the instant of ignition (t_v = 1 ms). Values of about 1.3 ± 0.2 m/s were attained at t = 1.001 s.

The turbulence level of the mist cloud during and after generation was also quantified for the three nozzle sets using different fluids and different air injection pressures.

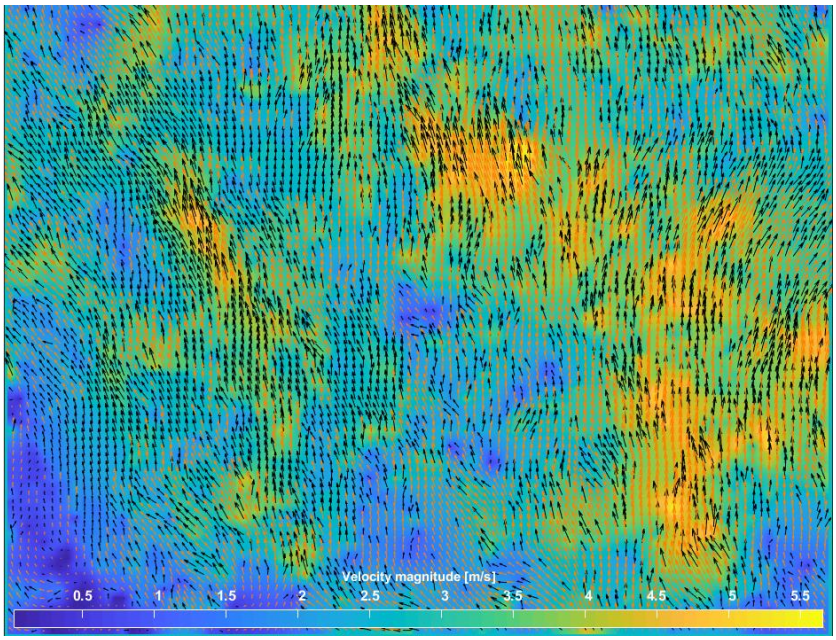

Figure 4: Spatial variation of the velocity magnitude of ethanol droplets at the end of the generation using nozzle set N' and P_{inj} = 3 bar

3.2 Evaporation model

The time-evolution of the diameter d of a hydrocarbon droplet during its evaporation is usually well represented by the d^2-law, initially proposed by Godsave (1953):

$$d^2 = d_0^2 - Kt \quad (4)$$

where K is the vaporization rate of the liquid and d_0 is the initial droplet diameter. Based on heat and mass balances applied on a single droplet, the d^2-law is valid for a spherical droplet of uniform temperature, steady in a quiescent environment. By equaling the vaporization mass rates obtained by both the heat and mass balances, the following relationship between the Spalding numbers can be deduced:

$$B_T = (1 + B_M)^{\frac{1}{Le}} - 1 \quad (5)$$

where B_T is the Spalding number related to thermal transfer, B_M is the Spalding number related to mass transfer and Le is the Lewis number defined as the ratio between the thermal and the mass diffusivities:

$$B_T = \frac{c_{pv}(T_\infty - T_d)}{L_v} \qquad (6)$$

$$B_M = \frac{Y_{vs} - Y_{v\infty}}{1 - Y_{vs}} \qquad (7)$$

with C_{pv}, the heat capacity of the vapor, Y_{vs}, its mass fraction at the droplet surface, $Y_{v\infty}$, its mass fraction in the surrounding gases, L_v, the vaporization enthalpy and T_∞ and T_d, the temperatures of the environment and of the droplet respectively. Y_{vs} is calculated by using the Clausius-Clapeyron equation at T_d. By assuming a d^2-law:

$$K = 8D\frac{\rho}{\rho_l} ln(1 + B_T) \qquad (8)$$

By solving the equations system (5 – 8), the time-evolution of droplet diameter can be deduced at various ambient temperatures, in addition to the evolution of the vapor/liquid ratio as a function of time. In a closed vessel, the saturation pressure at a given temperature should also be considered to define the characteristics of the mist. The assumption of a quiescent environment is obviously a strong one when dealing with the mists generated in the 20L sphere, as demonstrated by PIV measurements. As a consequence, equation (8) can be replaced by the following relationship for a turbulent cloud (Gökalp et al., 1992):

$$K_t = 8D\frac{\rho}{\rho_l} ln(1 + B_T) . \left(1 + 0.0276 Re^{\frac{1}{2}} Sc^{\frac{1}{3}}\right) \qquad (9)$$

where Sc is the Schmidt number and Re the droplet Reynolds number, deduced from PIV data. Similar approaches, both in quiescent or turbulent environments, can be used to represent the

evaporation of a droplet during its combustion. To take the combustion enthalpy Q and the oxygen mass fraction $Y_{Ox,\infty}$ into account, the Spalding numbers have to be modified accordingly:

$$B_T = \frac{c_{pv}(T_\infty - T_d) + \frac{Q}{s}Y_{Ox,\infty}}{L_v} \qquad (10)$$

$$B_M = \frac{Y_{vs} - \frac{Y_{Ox,\infty}}{s}}{1 - Y_{vs}} \qquad (11)$$

where s is a mass stoichiometric coefficient.

Figure 5 shows the time-evolution of the droplet size for the three fuels, considering a turbulent environment representative of that obtained before the ignition of the mist at 300K, 350K, 500K (no combustion) and, for diesel, at 500K by taking the combustion contribution into account (equations 10 and 11). The latter value was chosen arbitrarily low, but at temperatures obtained during a mist explosion, the combustion contribution on the evaporation dynamic would have been neglectable. It should be highlighted that, even if ethanol has a higher vapor pressure at a given temperature than diesel or Jet A1, its evaporation enthalpy is at least 3 times greater than for the other selected fuels. As a consequence, its evaporation rate at 300K lies between those of diesel and kerosene. For the latter fuel, for an initial diameter of 85 µm, a droplet will reach half of this value after approximately 60 ms. Consequently, a few milliseconds after its generation, a mist is still present in the 20L sphere. The temperature effect over the evaporation dynamics is significant and the vaporization of a diesel droplet occurs almost instantaneously at 500 K. Nevertheless, it should be kept in mind that such models represent the behavior of a single droplet and do not consider the saturation effect due to the vaporization of neighboring droplets in a closed sphere. This point will be addressed in 3.4.3.

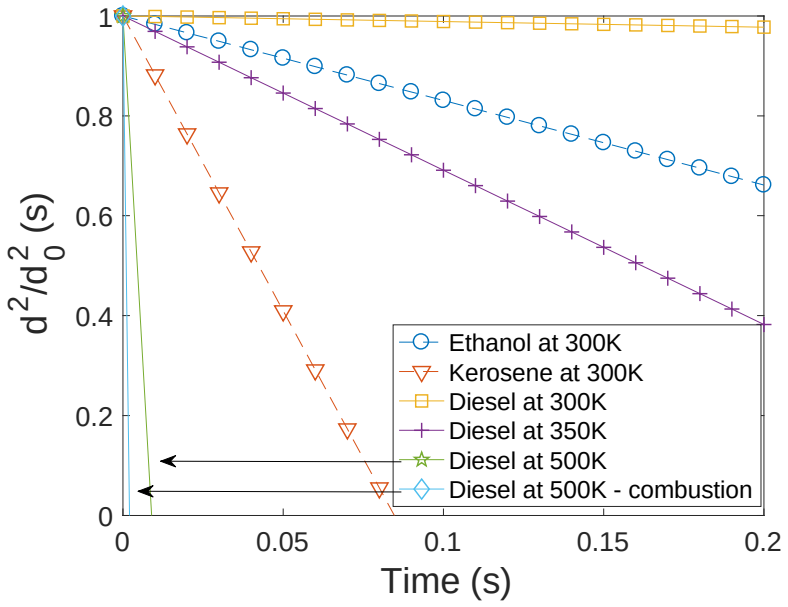

Figure 5: Influence of the temperature and hydrocarbon nature on the evaporation rate of 85 µm droplets

3.3 Ignition sensitivity

The lowest concentration of a mixture at which a propagation of a flame is supported away from the ignition source is defined as the Lower Explosive Limit (LEL). Burgoyne (1957) stated that the lower explosive limit of hydrocarbon mists, specifically tetralin, is around 50 g/m^3. Similarly, Britton and Harrison (2018) indicated a value of 40 g/m^3. In 1995, Eckhoff concluded that the LEL of a spray will range between 100 g/m^3 and 500 g/m^3 regardless of the fuel volatility (Eckhoff, 1995). Dufaud et al. (2015) also found a LEL in the order of 250 g/m^3 for lube oil mists. It should be noted that LEL values can be influenced when using different experimental apparatuses or different ignition sources (Gant, 2013). It should also be noted that a single average diameter is

often given in order to describe the whole DSD, whereas it can greatly vary as a function of the turbulence and time due to coalescence phenomenon.

For a d_{50} ranging from 8 to 10 µm, the LEL of the three selected fluids was determined in the MIST sphere following the explosion pressure rise. Results are presented in the table below:

Table 3. Results for the lower explosive limit (LEL) for ethanol, Jet A1 and diesel

Explosive limits	Ethanol 96%	Aviation fuel Jet A1	Diesel
LEL (g/m^3)	77 ± 5	94 ± 5	93 ± 5
LEL_{mist} ($\%_{v/v}$)	3.4	1.2	1.1
$LEL_{vapor\text{-}air}$ ($\%_{v/v}$)	3.3	0.6	0.5

In order to compare LEL of mists with LEL of vapors, mists were assumed to fully evaporate at the very moment of ignition allowing the calculation of LEL in $\%_{v/v}$. With regard to Section 3.2, this is obviously not the case, at least, in absence of ignition source. Results have shown that fuel mists of 8 – 10 µm are just as sensitive to explosion as their vapor phase in the same range of concentration. Such result tends to validate the statement that when a mist cloud is composed of droplets of diameters less than 10 µm, their flammability limits approach those of their corresponding vapor-air mixture (Burgoyne and Cohen, 1954; Faeth and Olson, 1968; Zabetakis, 1964).

The influence of the droplet size should be discussed. As stated by Gant (2013), the LEL of a mist is linked to the size of the droplets. In fact, Burgoyne (1963) studied the effect of the droplet size on the lower limit of flammability and showed that in upward flame propagation tests, the LEL

values tend to decrease with increasing drop diameter; however, with a downward flame propagation, such indications become harder to pinpoint with increasing drop diameters due to the presence of droplets falling vertically downwards. Tests on kerosene JetA1 mists generated with the three nozzle sets and ignited with 100 J chemical ignitors (Sobbe) showed that as the DSD increases, it becomes harder to ignite the mist cloud and hence the LEL increases (Table 4), a result which is consistent with that found by Zabetakis (1964).

Table 4. Effect of the DSD on the LEL of kerosene Jet A1 mists

Nozzle set	Mist DSD range (µm)	LEL (g/m^3)
N1	8-10	94 ± 5
N’	40-60	127 ± 5
N2	60-100	219 ± 5

The minimum ignition energy (MIE) is the smallest amount of spark energy needed to ignite the most easily ignitable mixture of a flammable substance in air. Such parameter is one of the most important parameters for the assessment of explosion risks and hazardous areas. In this study, attention was paid on the LEL. Nevertheless, preliminary MIE measurements were performed on fuel mist clouds using a high-voltage spark ignition system. It was designed to control the voltage and measure both the continuous current delivered and the real spark duration, which allow an accurate calculation of the ignition energy. For instance, first results show that the MIE of a turbulent Jet A1 mist cloud generated in the 20L sphere, of average diameters of 8 – 10 µm, lies between 300 and 330 mJ, which is consistent with values found by Ballal and Lefebvre (1978) for hydrocarbon mists.

3.4 Explosion severity

3.4.1 Validation tests

As presented in Section 2.5, the 20 L sphere was modified to allow the generation of mists and chemical ignitors of 100 J were used as ignition source. In accordance with the European standard PR EN15967:2020 "Determination of the maximum explosion pressure and maximum rate of pressure rise of gases and vapors", a MATLAB program was prepared to determine P_{max} as well as the maximum rate of pressure rise dP/dt_{max} using both two-point and five-point derivatives.

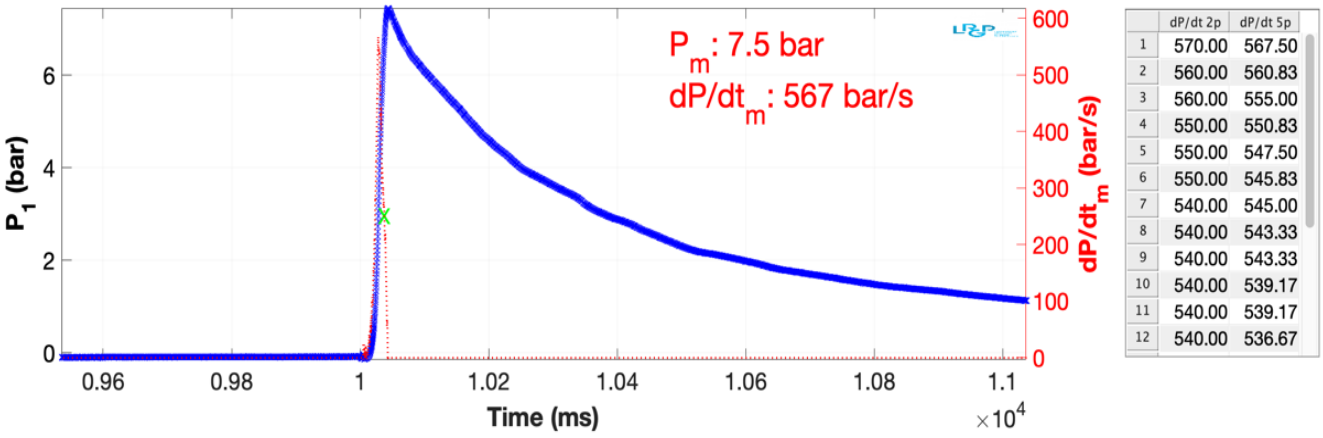

Figure 6. Time evolution of the explosion pressure of ethanol mist in the 20L explosion sphere (generation at ambient temperature using nozzle set N1)

Preliminary tests were performed on ethanol to calibrate the test method used. They show that the maximum explosion pressure reaches 7.5 barg, whereas the maximum rate of pressure rise reaches

567 bar/s (Figure 6) for an ethanol mist concentration of 128 g/m^3 (6.3%$_{v/v}$) of a DSD of about 8 - 10 µm generated by the nozzle set N1 with an injection pressure of 3 bar and at ambient temperature. These values are in good agreement with Mitu and Brandes (Mitu and Brandes, 2017) who found an absolute maximum explosion pressure of about 8 bar for an explosion of vapor ethanol/air mixture with a fuel/air ratio $\varphi = 1.15$ (about 137 g/m^3).

Chemical Equilibrium with Applications (CEA) was also used as a comparison tool between experimental results and theoretical calculations of liquid or gas phase combustion. Numerical data on the combustion of ethanol at different fuel/air ratios were obtained using CEA (Figure 7). Such results are consistent as the explosions performed in the MIST sphere are not under adiabatic conditions; therefore, it is normal to obtain an experimental P_{max} well below the theoretical adiabatic overpressure. Figure 7 also shows that tests were at least performed up to the stoichiometric concentration. The use of the CEA program permits to obtain theoretical equilibrium compositions of combustion products which can help in modeling mist explosions more finely.

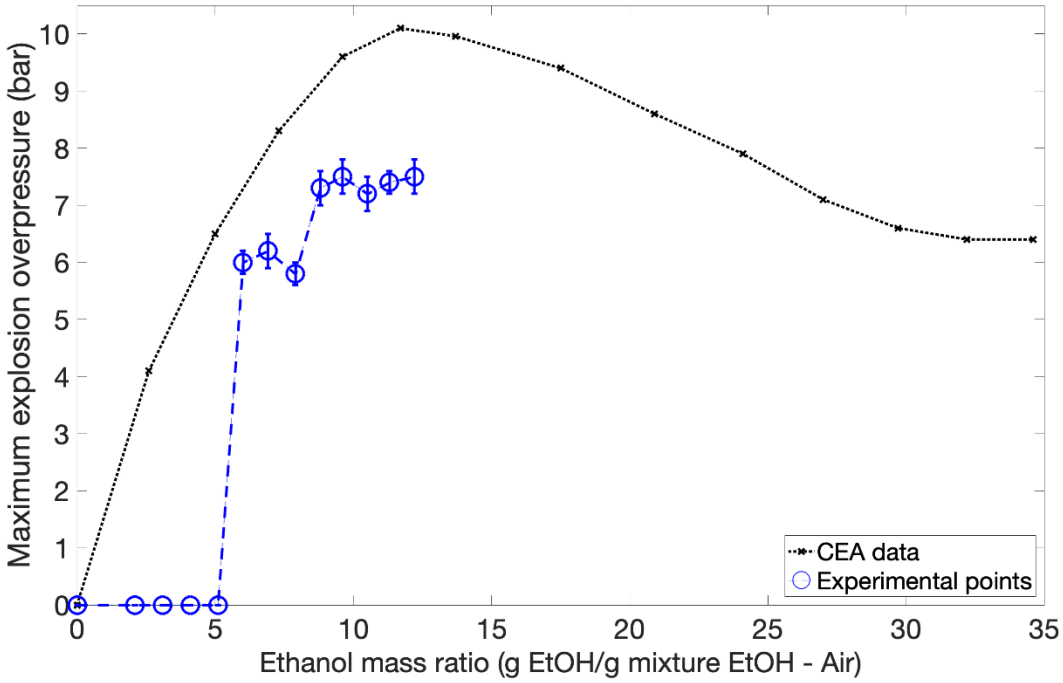

Figure 7. Comparison between theoretical CEA overpressure values and experimental results

3.4.2 Effect of the chemical nature of the fluid

The three fluids presented in Section 2.1 were tested under the same injection conditions (nozzle set N1, T = 27 °C, P_{inj} = 3 bar) and using the same 100 J chemical ignitors. Figures 8 and 9 present the variation of both the maximum explosion pressure and the maximum rate of pressure rise for diesel fuel, kerosene Jet A1, and ethanol. It should be noted that the lines are only arbitrary point-to-point connections and that a fitting will be adopted later on. As it can be seen, in the figures below, the three mists behave very differently once ignited. For ethanol, a maximum value of P_{max} of 7.5 barg and a maximum rate of pressure rise of 567 bar/s were found at a mist concentration of 128 g/m^3. However, in the case of kerosene Jet A1, 6.4 barg for P_{max} and 356 bar/s for dP/dt_{max} were found at a mist concentration of 159 g/m^3, which is consistent with tests performed by Zheng et al. (2014) on high flash point jet fuels (RP-5 and RP-3) resulting in values of about 6.5 bar as

P_{max}. As for diesel fuel mists, even though their values of rate of pressure rise are not much elevated, it can be seen that diesel can indeed ignite and produce an explosion at a temperature well below its flashpoint. Other than the different explosion behaviors, it can be seen the explosivity tends to decrease when passing from ethanol to Jet A1 and then to diesel mists. One explication to such decrease can be the difference in volatility of the three fluids as the vapor pressures at 20°C of ethanol, kerosene Jet A1, and diesel fuel are 5.9, 2, and 0.4 kPa respectively. Such influence was also found by Yuan et al. (2019) while testing the explosivity of n-octane and n-dodecane. More generally, as seen in Figure 5, the rate of vaporization of the fuels, depending notably on its heat capacity, vaporization and combustion enthalpies, should also be considered.

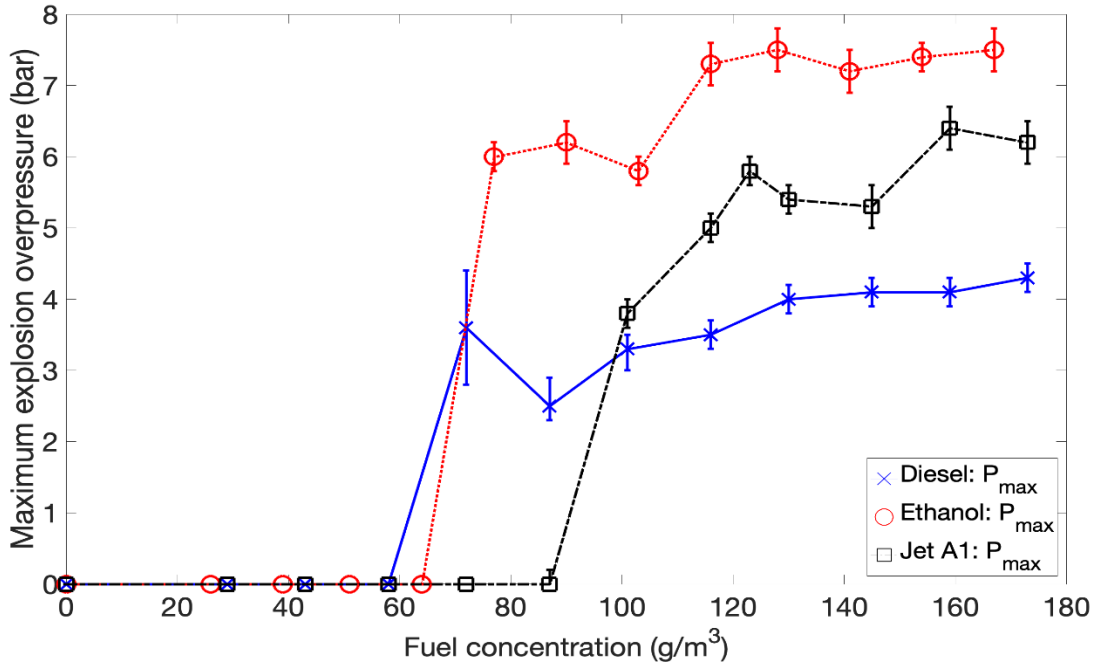

Figure 8. Variation of the maximum overpressure as a function of fuel concentrations in the 20L sphere (generation at ambient temperature using nozzle set N1)

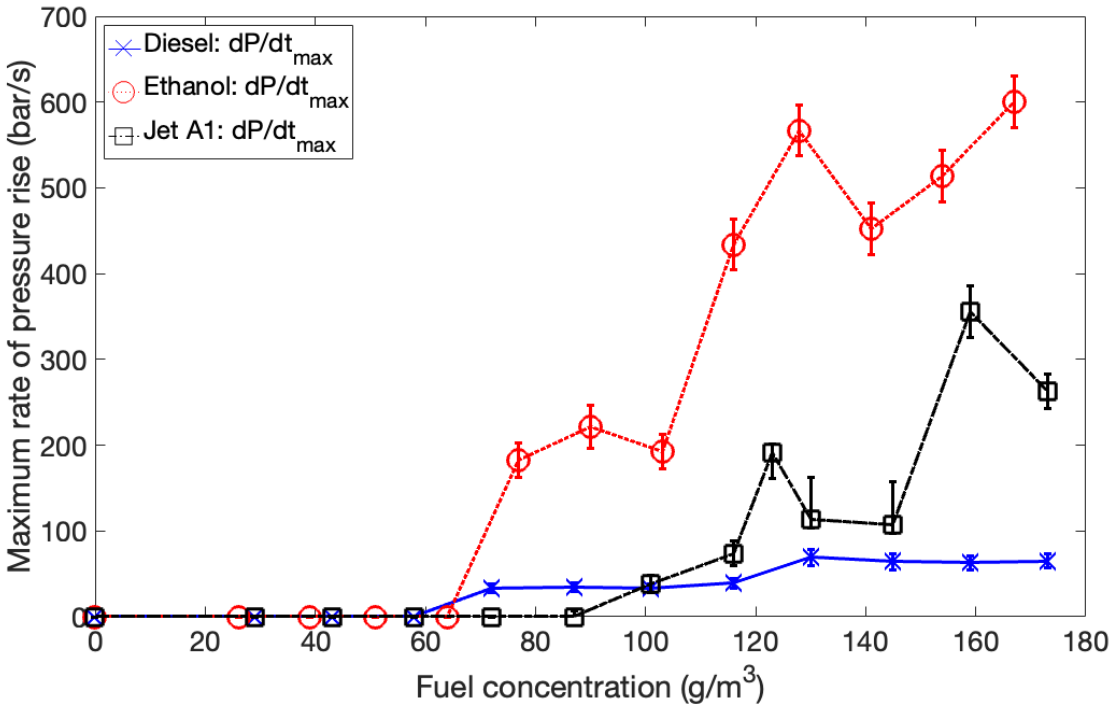

Figure 9. Variation of the maximum rate of pressure rise as a function of fuel concentrations in the 20L sphere (generation at ambient temperature using nozzle set N1)

3.4.3 Effect of the ambient temperature

The MIST sphere is equipped with a water jacket to control its temperature. To study the influence of the ambient temperature on the explosion severity of mists, the temperature of the sphere was notably increased from 20 °C to 40 °C, 60 °C and 80 °C for diesel mists. Tests were performed at various concentrations with pyrotechnical ignitors at 100 J. Results showed how ambient conditions can affect the rate of explosion pressure rise from values of about 53 bar/s at T = 20°C to about 493 bar/s at T = 80°C at a mist concentration of 115 g/m^3. This change can be explained by an increase of the vapor concentration around the droplet before ignition, reaching the lower explosive limit. The ignition step is then governed by a gas combustion regime and is not limited by the droplet evaporation as it is the case at 20°C. It can be seen in Figures 10 and 11 that this

effect is more pronounced on the maximum rate of pressure rise than on the maximum explosion pressure, highlighting the impact of the temperature on the mist combustion kinetics. Comparing the results obtained at 20 °C and those obtained at 27 °C (Figures 8 and 9), it can also be seen that a slight change in temperature causes variations in experimental values highlighting the importance of controlling the sphere temperature while performing experiments.

In addition to the augmentation of the sphere's temperature, pyrotechnical ignitors of high energies (1, 2, 5, and 10 kJ), which permit to increase the temperature locally, were tested. The results were consistent with that obtained by increasing the sphere's temperature, suggesting a relationship between the two parameters, even if the impact of chemical ignitors of different energies on the initial turbulence should not be neglected.

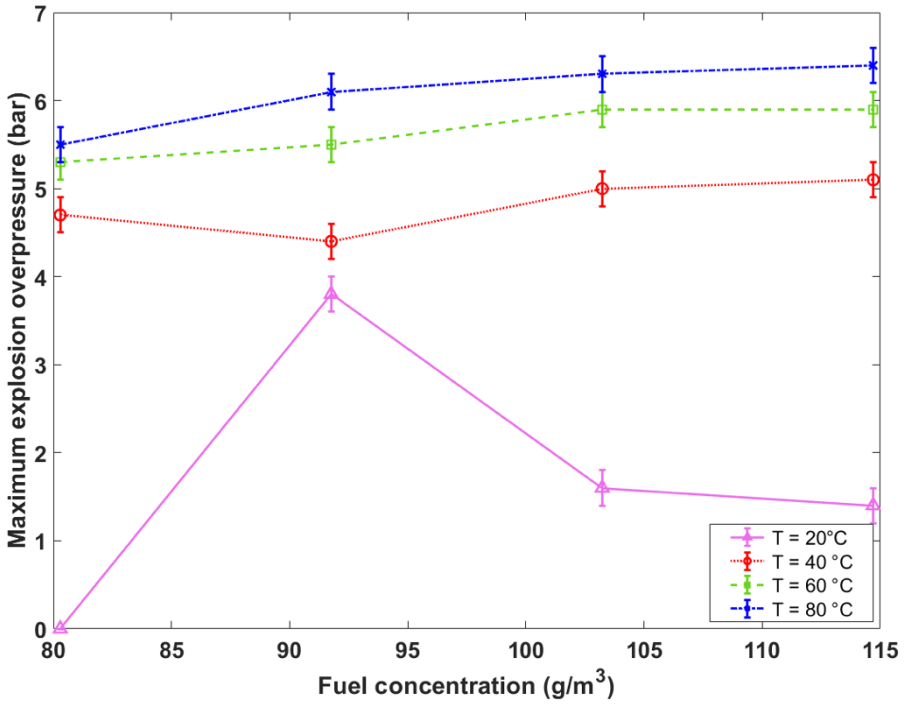

Figure 10. Variation of the maximum overpressure as a function of diesel mist concentrations in the 20L sphere at different temperatures (generation using nozzle set N1)

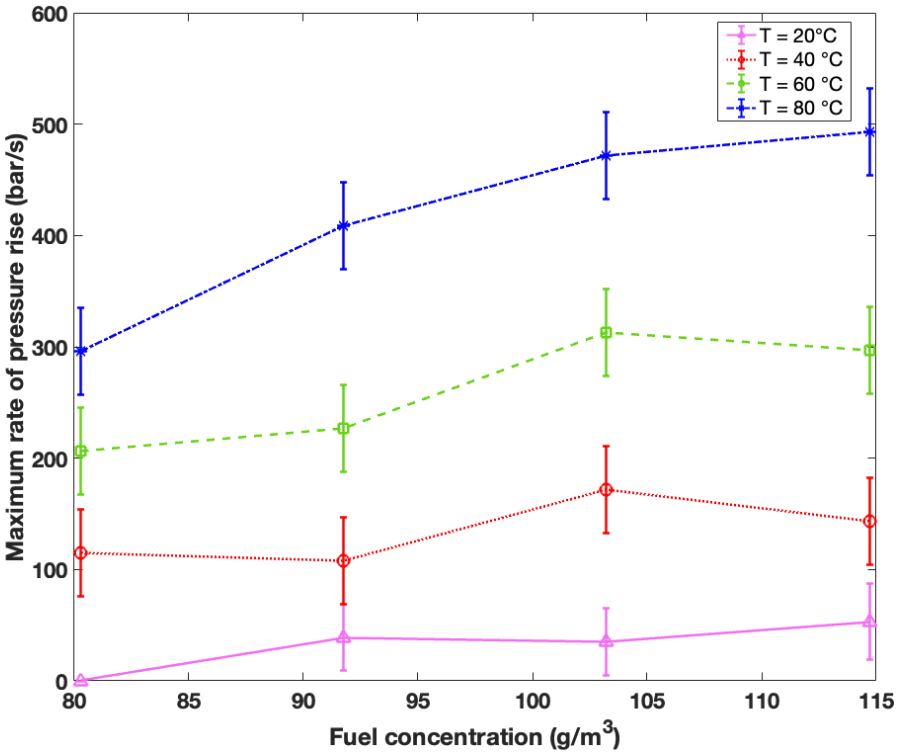

Figure 11. Variation of the rate of pressure rise as a function of diesel mist concentrations in the 20L sphere at different temperature (generation using nozzle set N1)

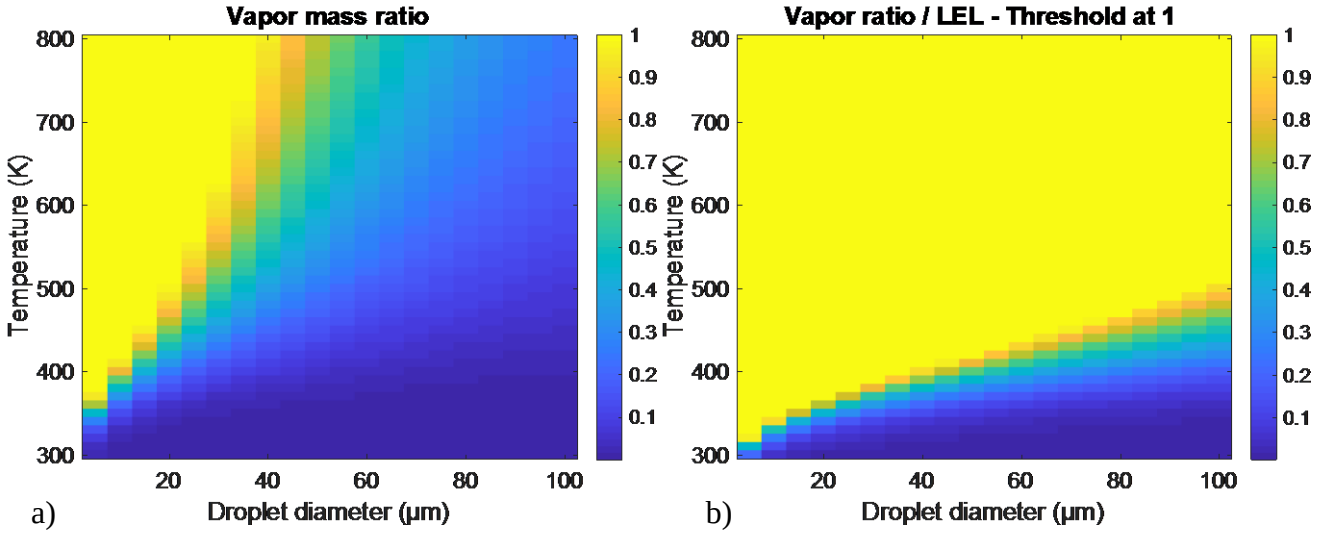

Figure 12. a) Evolution of the vapor mass ratio and of b) the normalized vapor ratio as a function of temperature and initial droplet size, for diesel mists – 4 g injected in the 20L sphere; 1 ms delay

The approach developed in Section 2.3 to model the evaporation of a single droplet was extended to the whole mist generated in the 20L sphere. It was assumed that each droplet of the mist vaporizes at the same rate; and both the saturation and the variation of the gas content as a function of the temperature were considered.

Figure 12a shows the mass proportion of the vapor in the diesel mist a millisecond after its generation in the sphere. It confirms that, for small DSD, the vapor content increases rapidly, especially above 353 K (80 °C), whereas it remains low for larger droplet sizes. For a nozzle set N1, for 8-10 µm droplets at 300 K, the vapor ratio is lower than 0.2 which may explain the low explosion pressures and maximum rate of pressure rises obtained for such mist. By considering the volume of the vapor generated by the mist evaporation and dividing it by $LEL_{vapor\text{-}air}$, a 'normalized vapor ratio' was defined. Figure 12b demonstrates that, even by neglecting the evaporation due to the presence of an ignition source, the vapor content is greater than the LEL when the mist is generated at 353 K (80 °C), which is not the case at 313K (40 °C) for instance. It should be noted that, for small droplets diameters, the LEL is reached at around 330 K (57 °C), which is consistent with diesel flashpoint. For droplet diameters ranging from 7 to 15 µm (typical DSD obtained with N1 nozzle) and at ambient temperature, the vapor mass fraction is not sufficient to reach the LEL instantaneously without the heat contribution of an ignition source. As a consequence, the combustion regime is not a fully homogeneous vapor phase combustion (transition regime) and the presence of vaporizing droplets can impact the flame propagation as demonstrated by Polymeropoulos (1984). When the initial temperature increases, the vapor fraction increases, promoting the vapor phase combustion. However, during the performed tests

tests, no explosion severity maximum was observed for the transition regime, as shown by Polymeropoulos (1984) for diesel mists (flame acceleration from 7 to 15 µm).

3.4.4 Effect of the Droplet Size Distribution

The droplet size distribution is one important parameter to be taken into account while studying the flammability and the explosion severity of a mist. Various authors considered that DSD is, more than other factors, directly related to the flame velocity and thus to the explosion severity (Danis et al., 1988; Yuan et al., 2019). But, in low-momentum sprays or quiescent mists, large droplets are affected by gravity and hence fall faster than smaller droplets, which tend to decrease the average mist mass concentration (Gant, 2013). Such effect can be seen in Table 5 where both the P_{max} and dP/dt_{max} decreased with increasing droplet size distribution. For concentrations of about 127 g/m^3 of jet A1 mists, the explosion pressure reached 5.6 bar in the case of nozzle set N1, 3.4 bar for nozzle set N', and no explosion occurred for nozzle set N2. The rate of pressure rise for the three considered cases were 162, 42, and 0 bar/s respectively. Such decrease in explosion severity can be explained by the decrease of the average surface area of the droplets cloud as their diameters increase for the same injected mass. It should also be kept in mind that, as shown by applying the model developed in Section 3.2 (for instance, Figure 12) decreasing the temperature and/or significantly increasing the DSD (beyond the transition region – 7 to 15 µm) will lead to a drop in the vapor mass fraction, which tends to lower the aerosol burning speed (Krishna et al., 2003; Polymeropoulos, 1984). Another explanation to these results is that, although ignition takes place in a rather turbulent mist cloud, large droplets may still be affected by gravity causing them to fall faster than smaller droplets and hence decreasing locally, especially near the ignition zone, the mist mass concentration. Other phenomena, such as radiative transfers in the mist and the

generation of soot at high fuel-air equivalence ratios should be considered. Moreover, during the flame propagation in the sphere, droplets can be projected against the sphere's inner wall leading to thermal quenching, which underlines the importance of scaling effects (Lian et al., 2011).

It should be noted that explosions did occur for nozzle set N2 reaching a P_{max} of 4.3 bar and a dP/dt_{max} of 70 bar/s for a mist concentration of 330 g/m^3. The influence of the total surface developed by the fuel in the mist is then stressed again, which confirms the relevance of choosing the Sauter mean diameter SMD as a major contributor of aerosol explosivity.

Table 5. Explosion severity of Jet A1 using the three nozzle sets for mist concentrations of about 127 g/m^3

Explosion severity	Nozzle set N1	Nozzle set N'	Nozzle set N2
P_m (barg)	5.6	3.4	0
dP/dt_m (bar/s)	162	42	0

4 Conclusion

This study aims to demonstrate that it is possible to characterize the ignition sensitivity and explosion severity of hydrocarbon mists with a single set-up. These tests should be performed on simple or/and standard equipment, which can be found in industries or laboratories, in order to be able to compare the results and propose adequate solutions for explosion risk management.

The work presented here allowed to conclude the following:

i. The Modified 20 L Ignition and explosion Severity Test (MIST) device, developed in this study, can be a suitable apparatus to assess mist explosivity and ignition sensitivity.

ii. Flammable fluids can indeed be ignited at temperatures well below their flashpoint when dispersed in a spray.

iii. Experiments carried out on ethanol, kerosene Jet A1, diesel, and other fuels which were not presented here (lube oil, biodiesel…) have allowed to validate the procedures and setups and show the influence of some operating conditions, such as the ambient temperature, the fuel equivalence ratio, and the droplet size distribution, on the safety parameters of hydrocarbon mists.

iv. The LEL of the three hydrocarbon mists was shown to be 77 g/m^3 ($3.3\%_{v/v}$), 94 g/m^3 ($1.2\%_{v/v}$) and 93 g/m^3 ($1.1\%_{v/v}$) for ethanol, Jet A1 and diesel mists respectively. Moreover, it was notably demonstrated that the LEL of Jet A1 mist increases with an increasing DSD.

v. The rate of pressure rise is also greatly influenced by the combustion kinetics and its rate-limiting step (evaporation, fuel oxidation…). The effect of the sphere temperature was also studied showing an increase in both P_m and dP/dt_m of diesel mist explosions when the temperature of the sphere was increased from 20 °C to 80 °C and thus highlighting the influence of the fuel phase (gas, gas-aerosol, liquid aerosol) before ignition. It was also shown that, over the tested diameter range, increasing DSD leads to a diminution of the explosion severity.

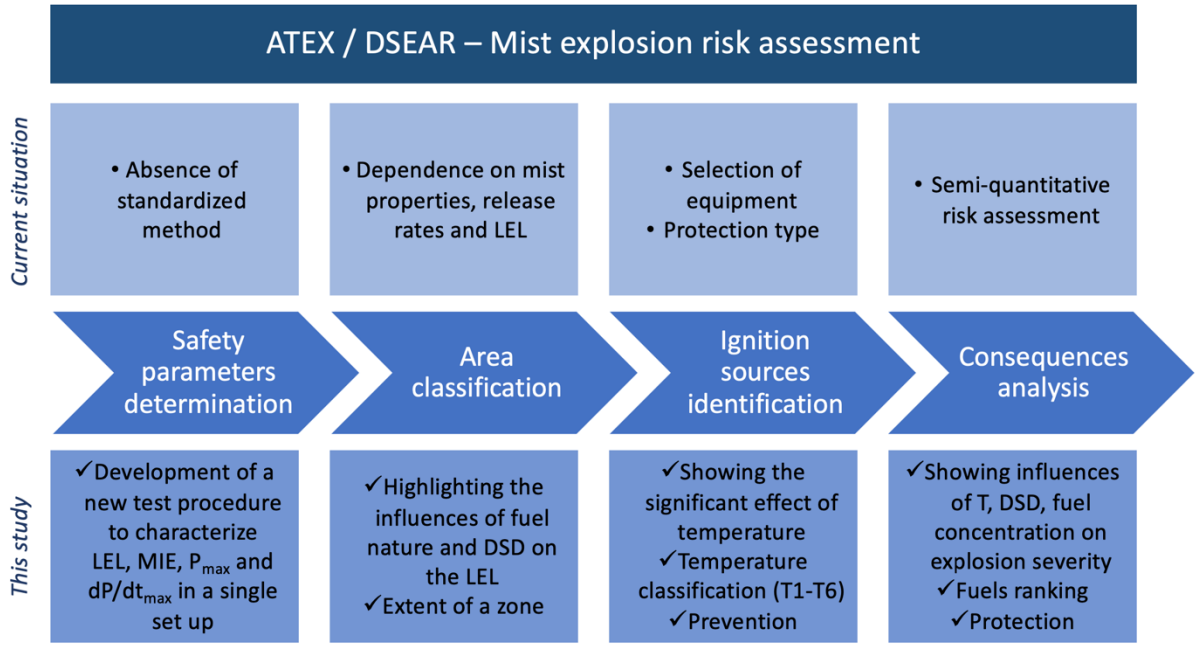

Figure 13. Summary of the practical applications of this study in terms of mist explosion risk assessment

Additional tests are currently being performed at various initial turbulence levels and on a larger range of DSD with several conventional fuels or hydrocarbons (e.g. iso-octane, biodiesel, light fuel oil, lube oil…). This experimental approach will be coupled with both CFD simulation, to better understand the hydrodynamics within the explosion vessel, and combustion modeling, to highlight the influence of the rate-limiting step of mist explosion on the safety parameters.

As shown by Figure 13, the practical applications of this work on mist explosion risk assessment are numerous, from the development of a new procedure allowing the determination of essential safety parameters for mists, to the possibility of fuel ranking for consequence analysis. These results also highlight the influence of aerosol dispersion conditions (temperature, DSD…) on their

flammability, and thus, on the potential extent of ATEX zones. Finally, this study sheds light on the importance of assessing fuel mist explosions, a risk that still may be misjudge or neglected as standards still need to be developed.

Acknowledgements

This work was supported financially by the French Ministry for the Ecological Transition and the French Ministry of Higher Education, Scientific Research and Innovation. The authors would also like to thank the Health and Safety Executive (UK) for the fruitful exchanges on the topic. The contents of the work, including any opinions and/or conclusions expressed, are those of the authors alone and do not necessarily reflect French Ministries policies.

5 References

Ballal, D.R., Lefebvre, A.H., 1976. Ignition and flame quenching of quiescent fuel mists. Proc. R. Soc. Lond. A 364, 277-294. https://doi: 10.1098/rspa.1978.0201

Ballal, D.R., Lefebvre, A.H., 1981. A general model of spark ignition for gaseous and liquid fuel-air mixtures. Proceedings of the eighteenth (international) symposium on combustion. 18, 1737–1746. https://doi.org/10.1016/S0082-0784(81)80178-6

Bowen, P.J., Shirvill, L.C., 1994. Combustion hazards posed by the pressurized atomization of high-flashpoint liquids. J. Loss Prev. Process Ind. 7, 233-241. https://doi.org/10.1016/0950-4230(94)80071-5

Britton, L.G., Harrison, B.K., 2018. Minimum explosible concentrations of mist and dust clouds. Process Saf. Prog. 37, 4-17. https://doi.org/10.1002/prs.11959

Burgoyne, J.H., 1963. The flammability of mists and sprays. Proceeding of the second symposium on chemical process hazards, 5.

Burgoyne, J.H., 1957. Mist and spray explosions. Chem. Eng. Prog. 53, 121–124.

Burgoyne, J.H., Cohen, L., 1954. The effect of drop size on flame propagation in liquid aerosols. Proceedings of the Royal Society of London. Series A, mathematical and physical sciences 225, 375-392.

Burrell, G., Gant, S., 2017. Liquid classification for flammable mists. RR1108 HSL report, UK.

Danis, A.M., Namer, I., Cernansky N.P. 1988. Droplet size and equivalence ratio effects on spark ignition of monodisperse N-heptane and methanol sprays. Combust. Flame, 74 (3), 285-294, https://doi.org/10.1016/0010-2180(88)90074-0.

Dufaud, O., Charvet, A., Mougel, G., Molière, M., Luthun, S., Brunello, D., Perrin, L., Delimoges, S., Couchot, M., 2015. Generation, characterization and ignition of lube oil mists. Proceedings of ASME Turbo Expo 2015, combustion, fuels and emissions. Montreal, Canada, No. GT2015-43524, V04BT04A039; 8 pages. https://doi.org/10.1115/GT2015-43524.

Eckhoff, R.K., 2016. Chapter five - Explosions of clouds of combustible liquid droplets in air, in: Explosion hazards in the process industries (second edition). Gulf Professional Publishing, 209-232. https://doi.org/10.1016/B978-0-12-803273-2.00005-0

Eckhoff, R.K., 1995. Generation, ignition, combustion and explosion of sprays and mists of flammable liquids in air: a literature survey. Offshore technology report OTN 95 260, Health and Safety Executive, UK.

Eichhorn, J., 1955. Careful! Mist can explode. Petroleum Refiner. 34(11), 194-196.

Energy Institute, 2015. Model code of safe practice: Area classification code for installations handling flammable fluids.

Faeth, G.M., Olson, D.R., 1968. The ignition of hydrocarbon fuel droplets in air. SAE Transactions 77, 1793-1802.

Fraser, R.P., Eisenklam, P., 1956. Liquid atomization and the drop size of sprays. Institution of Chemical Engineers. 34(4): 294.

Gant, S., 2013. Generation of flammable mists from high flashpoint fluids: literature review. Research Report RR980, Health and Safety Executive, UK.

Godsave, G.A.E., 1953. Studies of the combustion of drops in a fuel spray-the burning of single drops of fuel. Proceedings of the (international) symposium on combustion. 4, 818-830. https://doi.org/10.1016/S0082-0784(53)80107-4.

Gökalp, I., Chauveau, C., Simon, O., Chesneau, X., 1992. Mass transfer from liquid fuel droplets in turbulent flow. Combust. Flame. 89, 286-298. https://doi.org/10.1016/0010-2180(92)90016-I.

Ji, C., Yuan, S., Jiao, Z., Huffman, M., El-Halwagi, M.M., Wang, Q., 2021. Predicting flammability-leading properties for liquid aerosol safety via machine learning. Process Saf. Environ. Prot., 148, 1357-1366. https://doi.org/10.1016/j.psep.2021.03.012

Kooij, S., Sijs, R., Denn, M.M., Villermaux, E., Bonn, D., 2018. What Determines the Drop Size in Sprays? Phys. Rev. X 8, 031019. https://doi.org/10.1103/PhysRevX.8.031019

Krishna, K., Rogers, W.J., Mannan, S.M. 2003. The use of aerosol formation, flammability, and explosion information for heat-transfer fluid selection. J. Hazard. Mater., 104 (1-3), 215-226, https://doi.org/10.1016/S0304-3894(03)00273-5.

Lees, P., Gant, S., Bettis, R., Vignes, A., Lacome, J.-M., Dufaud, O., 2019. Review of recent incidents involving flammable mists. Proceedings of IChemE Hazards 29 Conference, Birmingham, UK, 23.

Lian, P., Ng, D., Mejia, A.F., Cheng, Z., Mannan, M.S. 2011. Study on flame characteristics in aerosols by industrial heat transfer fluids. Ind. Eng. Chem. Research, 50 (12), pp. 7644-7652. https://doi.org/10.1021/ie200179y.

Mitu, M., Brandes, E., 2017. Influence of pressure, temperature and vessel volume on explosion characteristics of ethanol/air mixtures in closed spherical vessels. Fuel. 203, 460-468. https://doi.org/10.1016/j.fuel.2017.04.124

Pinheiro, A.P., Vedovoto, J.M., da Silveira Neto, A., G.M. van Wachem, B., 2019. On ethanol droplet evaporation in the presence of background fuel vapor. Proceedings of ILASS–Europe 2019, 29th Conference on liquid atomization and spray systems, 2-4 September, Paris, France.

Polymeropoulos, C.E., 1984. Flame propagation in aerosols of fuel droplets, fuel vapor and air Combust. Sci. Technol., 40 (5-6), 217-232, https://doi.org/10.1080/00102208408923807.

Santandrea, A., Gavard, M., Pacault, S., Vignes, A., Perrin, L., Dufaud, O., 2020. 'Knock on nanocellulose': Approaching the laminar burning velocity of powder-air flames. Process Saf. Environ. Prot. 134, 247–259. https://doi.org/10.1016/j.psep.2019.12.018

Santon, R.C., 2009. Mist fires and explosions - an incident survey. IChemE Hazards XXI Symposium & Workshop, Manchester, UK.

Skjold, T., 2003. Selected aspects of turbulence and combustion in 20-litre explosion vessels : development of experimental apparatus and experimental investigation. Master thesis, University of Bergen, Norway.

ST/SG/AC.10/30/Rev.8, 2019. Globally harmonized system of classification and labelling of chemicals (GHS)., 8th revised version. ed. United Nations, New York and Geneva.

Thielicke, W., 2021. PIVlab - particle image velocimetry (PIV) tool with GUI (online document). GitHub. url https://github.com/Shrediquette/PIVlab/releases/tag/2.53 (accessed 7.1.21).

Thimothée, R., 2017. Experimental characterization of a laminar flame propagation in a two-phase medium (aerosol) in microgravity conditions. PhD thesis, Université d'Orléans, France.

Torrado, D., 2017. Effect of carbon black nanoparticles on the explosion severity of gas mixtures. PhD thesis, Université de Lorraine, France.

Yuan, S., Ji, C., Han, H., Sun, Y., Mashuga, C.V., 2021. A review of aerosol flammability and explosion related incidents, standards, studies, and risk analysis. Process Saf. Environ. Prot. 146, 499–514. https://doi.org/10.1016/j.psep.2020.11.032

Yuan, S., Ji, C., Monhollen, A., Kwon, J.S.I., Mashuga, C., 2019. Experimental and thermodynamic study of aerosol explosions in a 36 L apparatus. Fuel. 245, 467-477. https://doi.org/10.1016/j.fuel.2019.02.078

Zabetakis, M.G., 1964. Flammability characteristics of combustible gases and vapors. No. BM-BULL-627, Bureau of Mines, Pittsburgh, United States. https://doi.org/10.2172/7328370

Zheng, L., Changbo, L., Gaojun, A., Chunhua, X., Youjie, Z., Lianling, R., Xudong, W., Lifeng, X., Gang, W., Feng, W., Limin, S., 2014. Comparative study on combustion and explosion characteristics of high flash point jet fuel. Procedia Engineering, Proceedings of the International symposium on safety science and technology. 84, 377-383. https://doi.org/10.1016/j.proeng.2014.10.447.